Frontiers of Information Technology & Electronic Engineering
www.jzus.zju.edu.cn; engineering.cae.cn; www.springerlink.com
ISSN 2095-9184 (print); ISSN 2095-9230 (online)
E-mail: jzus@zju.edu.cn

On-chip optical interconnect using visible light*

Wei CAI[1,2], Bing-cheng ZHU[1], Xu-min GAO[1], Yong-chao YANG[1], Jia-lei YUAN[1], Gui-xia ZHU[1], Yong-jin WANG[†‡1], Peter GRÜNBERG[1]

([1]*Peter Grünberg Research Center, Nanjing University of Posts and Telecommunications, Nanjing 210003, China*)

([2]*School of Computer Engineering, Nanjing Institute of Technology, Nanjing 211167, China*)

[†]E-mail: wangyj@njupt.edu.cn

Received Nov. 18, 2016; Revision accepted Mar. 14, 2017; Crosschecked Sept. 30, 2017

Abstract: We propose and fabricate a monolithic optical interconnect on a GaN-on-silicon platform using a wafer-level technique. Because the InGaN/GaN multiple-quantum-well diodes (MQWDs) can achieve light emission and detection simultaneously, the emitter and collector sharing identical MQW structure are produced using the same process. Suspended waveguides interconnect the emitter with the collector to form in-plane light coupling. Monolithic optical interconnect chip integrates the emitter, waveguide, base, and collector into a multi-component system with a common base. Output states superposition and 1×2 in-plane light communication are experimentally demonstrated. The proposed monolithic optical interconnect opens a promising way toward the diverse applications from in-plane visible light communication to light-induced artificial synaptic devices, intelligent display, on-chip imaging, and optical sensing.

Key words: Homogeneous integration; Multiple-quantum-well diode; Visible light interconnection; Coexistence of light emission and photodetection

https://doi.org/10.1631/FITEE.1601720 **CLC number:** TN491; E963

1 Introduction

A light-induced transistor can be formed by combining a light-emitting diode (LED) and a photodiode with a common n-contact as the base on the same substrate. The light emitted from the LED can be collected by the closely coupled photodiode (van Zeghbroeck *et al.*, 1989; Feng *et al.*, 2004; Zhang *et al.*, 2014; Cai *et al.*, 2016a). The light-induced transistor is similar to a bipolar transistor except that photons rather than electrons are used to transmit signals. There are six escape cones for a planar LED (Schubert *et al.*, 2005). Two of these cones are out-of-plane, and the remaining four are in-plane. The in-plane escape cones can be considered as waveguides to guide the emitted light with controllable propagation directions. Therefore, data transport simultaneously occurs when the emitted light of a planar LED is modulated. Correspondingly, there are six incoming interfaces for a planar photodiode. A variety of possible output combinations can be achieved by integrating different light-induced transistors with a common base and collector, in which every emitter can be adopted as an independent transmitter. The electron-to-photon conversion is realized at the emitter, the collector completes the photon-to-electron conversion, and data transport is achieved through light coupling rather than across short electrical wires (Sato *et al.*, 2015; Sun *et al.*, 2015), and this is promising for managing the heating effect in high-density microchips.

Among the semiconductors used in present-day optoelectronic devices, GaN-based materials have simultaneously the selectable functionalities of light emission, transmission, and photodetection (Jhou

‡ Corresponding author

* Project supported by the Special Project for Inter-government Collaboration of State Key Research and Development Program, China (No. 2016YFE0118400), the Natural Science Foundation of Jiangsu Province, China (No. BE2016186), the National Natural Science Foundation of China (Nos. 61322112 and 61531166004), the Research Project (Nos. KYZZ16_0258, CJKA201506, and CKJA201306), and the '111' Project

ORCID: Yong-jin WANG, http://orcid.org/0000-0001-8109-4640

et al., 2005; Brubaker *et al.*, 2013; Tchernycheva *et al.*, 2014). GaN-based LEDs and photodiodes can be fabricated using the same technology (Jiang *et al.*, 2014; Li *et al.*, 2015; Cai *et al.*, 2016b). Over time, advancements in the epitaxial growth of GaN have enabled high-quality p-n junction GaN-based multiple quantum wells (MQWs) to be deposited on silicon substrates (Krost and Dadgar, 2002; Triviño *et al.*, 2015). The GaN-on-silicon platform can meet the requirements for mass production of the monolithic optoelectronic integration, which combines different optoelectronic elements on the same chip. The device limitations caused by the thick epitaxial films can be overcome using the mature silicon removal process and back-wafer etching of a suspended membrane (Li *et al.*, 2014), creating improved performance for integrated optoelectronic devices (Noda and Fujita, 2009; Wierer *et al.*, 2009). Furthermore, the light emitted by a GaN-based emitter can be controlled by tuning the indium or aluminum contents in GaN-based MQWs (Kuykendall *et al.*, 2007; Qian *et al.*, 2008; Chen *et al.*, 2011).

In the present paper, we report the realization of a monolithic integration of the emitter, waveguide, and photodiode on a single chip, which is fabricated using a wafer-level technique. The integrated device originates from a combination of two light-induced transistors, in which suspended waveguides are used for light coupling. The light from the emitter rather than electrons is transported through the waveguide to the collector, which leads to an induced photocurrent. The possible output combinations are investigated for potential on-chip optical interconnect using visible light.

2 Fabrication of the integrated device

The proposed optoelectronic device consists of emitter and collector, such that the fabrication technology for creating this device is identical to that for creating the LED and photodiode. A wafer-level technique is developed to manufacture the monolithic integrated device on a 2-inch GaN-on-silicon platform (Bai *et al.*, 2016; Wang *et al.*, 2016; Yuan *et al.*, 2016), which is composed of a 220-nm-thick p-GaN layer, a 250-nm-thick InGaN/GaN MQW, a 3.2-μm-thick n-GaN layer, a 400-nm-thick undoped GaN layer, a 900-nm-thick Al(Ga)N buffer layer, and a 200-μm-thick silicon substrate. The top layer is first defined and etched down to n-GaN to form a mesa by inductively coupled plasma reactive ion etching (ICP-RIE) with Cl_2 and BCl_3 hybrid gases at flow rates of 10 and 25 sccm, respectively. Using the lift-off technique, 20 nm Ni/180 nm Au bilayers are evaporated onto the surface of the p-GaN and n-GaN layers, and p- and n-contacts are formed after annealing at 500 °C in a N_2 atmosphere for 5 min. The waveguides are then patterned and etched with a depth of 3.6 μm by ICP-RIE. The top device structures are protected by a photoresist, and then the silicon substrate is spin-coated with a photoresist and patterned by backside alignment photolithography. Both silicon removal and back-side thinning of the suspended membrane are conducted to obtain membrane-type optoelectronic devices on a 3-μm-thick suspended membrane.

The schematic of the suspended optoelectronic device is illustrated in Fig. 1a. One n-electrode is shared by devices A, B, and C. Sharing the n-electrode is beneficial to the miniaturization of the integrated device, which is crucial to further high-density microchips. The p-electrodes with a diameter of 70 μm are fabricated on the mesa in the suspended-membrane region. Three suspended waveguides that are 80-μm long, 3-μm high, and 10-μm wide are used for device connections. The common n-contact serves as the base. Device C acting as the photodiode is the common collector when device A or B (or both) is (are) used as the emitter(s). On the other hand, device C operating under LED mode becomes the common emitter when device A or B (or both) is (are) used as the collector(s). When the LEDs are turned on, photons are transported through the waveguides and absorbed in the photodiode, inducing photocurrent. Fig. 1b presents the light emission images when device A operating under LED mode is injected with a current of 800 μA and device B is off. The p-electrode region is dark because the thick metal contact suppresses the light emission. Fig. 1c presents the light emission images for both devices A and B under LED operation with the same injection current of 800 μA. For a suspended device, the emitted light could be confined and guided as waveguide modes due to the large index contrast between GaN and air (Sekiya *et al.*, 2015; Shokhovets *et al.*, 2015). The guided light propagates inside the suspended membrane and enters the air at the mesa and isolation trench facets.

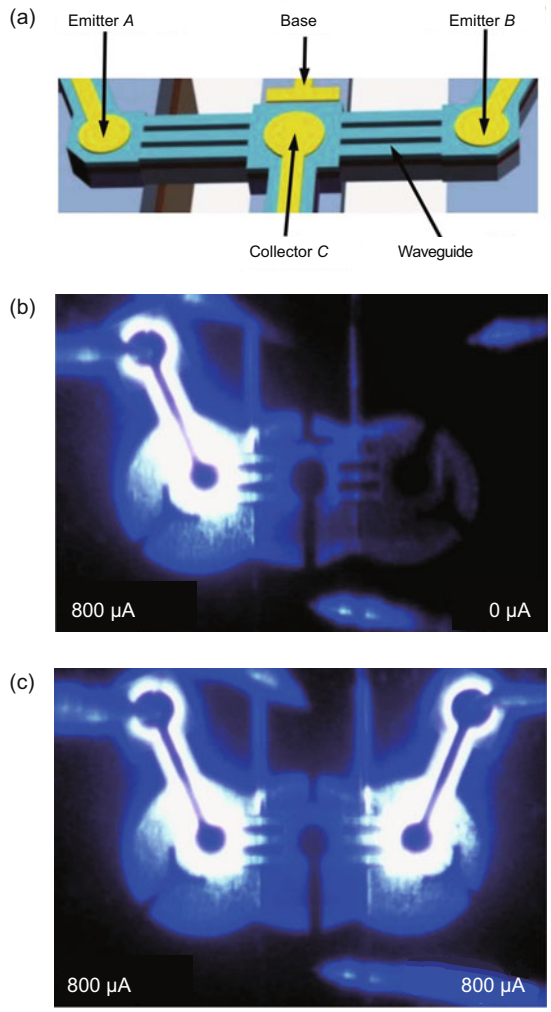

Fig. 1 Schematic of the proposed optoelectronic devices (a), light emission image when device *A* is under emitter operation and device *B* is off (b), and light emission image when both devices *A* and *B* are under emitter operation at 800 μA (c) (References to color refer to the online version of this figure)

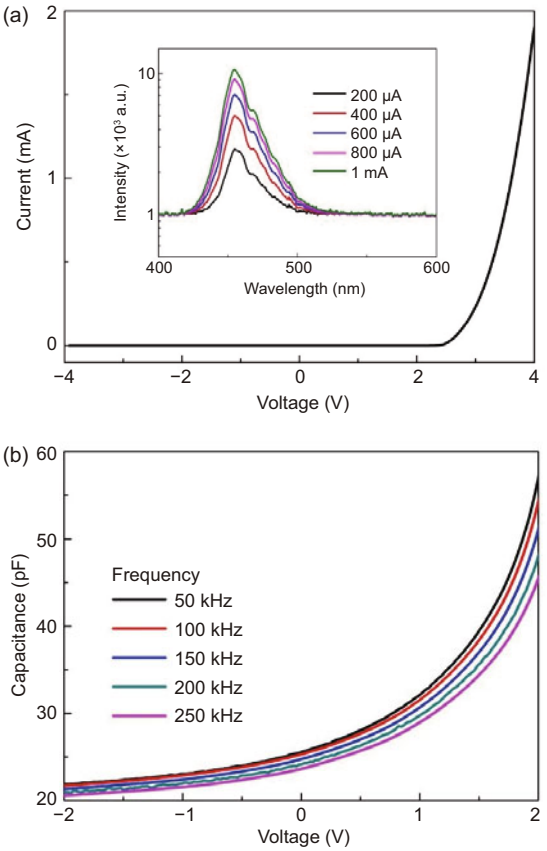

Fig. 2 Measured current-voltage (*I*-*V*) plot of device *C* (a) with the inset showing the EL spectra measured at different injection current levels, and the frequency-dependent capacitance-voltage (*C*-*V*) plot of device *C* operating under photodiode mode (b) (References to color refer to the online version of this figure)

3 Experimental results and discussion

The typical current-voltage performance of the suspended emitter is measured using an Agilent B1500A semiconductor device analyzer. Fig. 2a shows the measured current-voltage (*I*-*V*) plot of the suspended emitter and it indicates that the turn-on voltage is approximately 2.5 V. The inset of Fig. 2a presents the measured log-scaled electroluminescence (EL) plots for the suspended emitter. As shown in the inset, since the light emission intensity is modulated by the injection current of the emitter (Vučić *et al.*, 2010; McKendry *et al.*, 2012; Liao *et al.*, 2014), the emission increases as the injection current increases from 200 μA to 1 mA, and the dominant EL peak is measured at 454.6 nm at the injection current of 1 mA. Fig. 2b shows the capacitance-voltage (*C*-*V*) behavior of device *C* at different frequencies from 50 to 250 kHz. The photodiode can be considered to be a parallel-plate capacitor when the bias voltage is lower than the turn-on voltage. Therefore, as a p-n junction diode, the width of the depletion region decreases as the bias voltage increases from −2 to 2 V, leading to an improved capacitance. The frequency dependence of the capacitance is clearly observed. In the bias range of 50 to 250 kHz, the measured capacitance decreases as the frequency increases.

The proposed device can be treated as a photonic integrated circuit composed of two emitters, a common collector, a common base, and suspended waveguides for light coupling to create two light-induced transistors with a common base region for

on-chip optical interconnect. When the emitters are operating, the guided light propagates along the suspended waveguides and is detected by the photodiode. Fig. 3 shows the induced photocurrent of the photodiode measured with the bias voltage in the range of −4 to 2 V. Fig. 3a show the induced photocurrent of the photodiode when the injection currents are applied to emitter A at levels ranging from 0 to 800 μA and when the injection current of emitter B is 0 μA. Because the light intensity is modulated by the injection current of the emitters, more light power is transported to the photodiode through the suspended waveguides with an increased injection current of the emitter, leading to an increased photocurrent. An increased photocurrent is observed with an increasing bias voltage of the photodiode from −4 to 2 V, which is consistent with the bias-voltage-dependent capacitance. Figs. 3b and 3c illustrate that, at the bias voltage of −4 V and when the injection current of emitter A is 0 μA, the initial photocurrents of the photodiode are clearly observed at −16 and −25 nA, when the injection current levels of emitter B are 200 and 400 μA, respectively. Furthermore, in Figs. 3a–3c, as the injection current of emitter B is increased from 0 to 400 μA, emitter B is under operation mode and provides a stable supply of photons, indicating that there will be an initial induced photocurrent when emitter A operates. Fig. 3d shows the measured photocurrent when the injection current of emitter A is 600 μA and the injection current levels of emitter B are increased from 0 to 800 μA. Fig. 3 indicates that the photons from different emitters can be accumulated.

To experimentally demonstrate that the proposed device works for on-chip optical interconnect, we need to confirm that the device can have four possible output combinations; namely, both emitters are turned off, emitter A operates with encoded output and emitter B is off, emitter A is off and emitter B is turn on for encoded output, and both emitters operate synchronously to output signals. As shown in Fig. 4a, both emitters are directly driven by an Agilent 33522A arbitrary waveform generator to modulate the emitted light, and the collector detects the guided light and completes photon-to-electron conversion. The bias voltage of collector C is 0 V, and the received electric signals are characterized using an Agilent DSO9254A oscilloscope without an amplifier and filtering process. The two emitters are driven

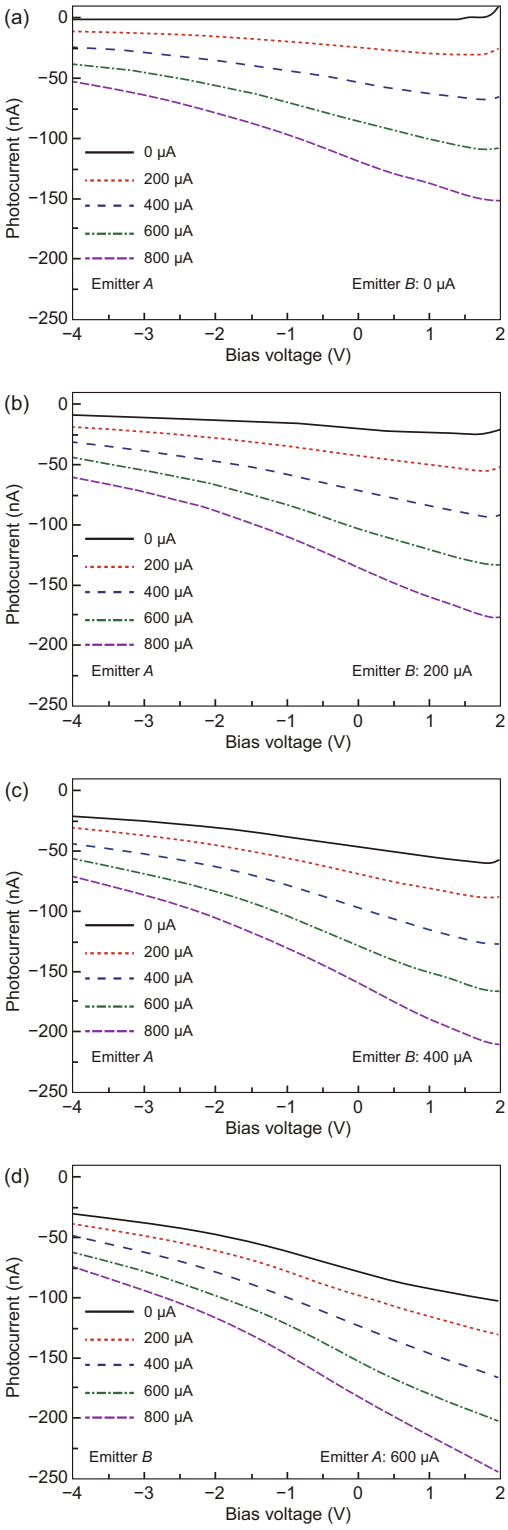

Fig. 3 Measured current-voltage (I-V) curves of the photodiode versus the injection current levels of emitter A ranging from 0 to 800 μA when the injection currents of emitter B are 0 μA (a), 200 μA (b), and 400 μA (c), and I-V curves of the photodiode versus the injection current of emitter B when the injection current of emitter A is 600 μA (d)

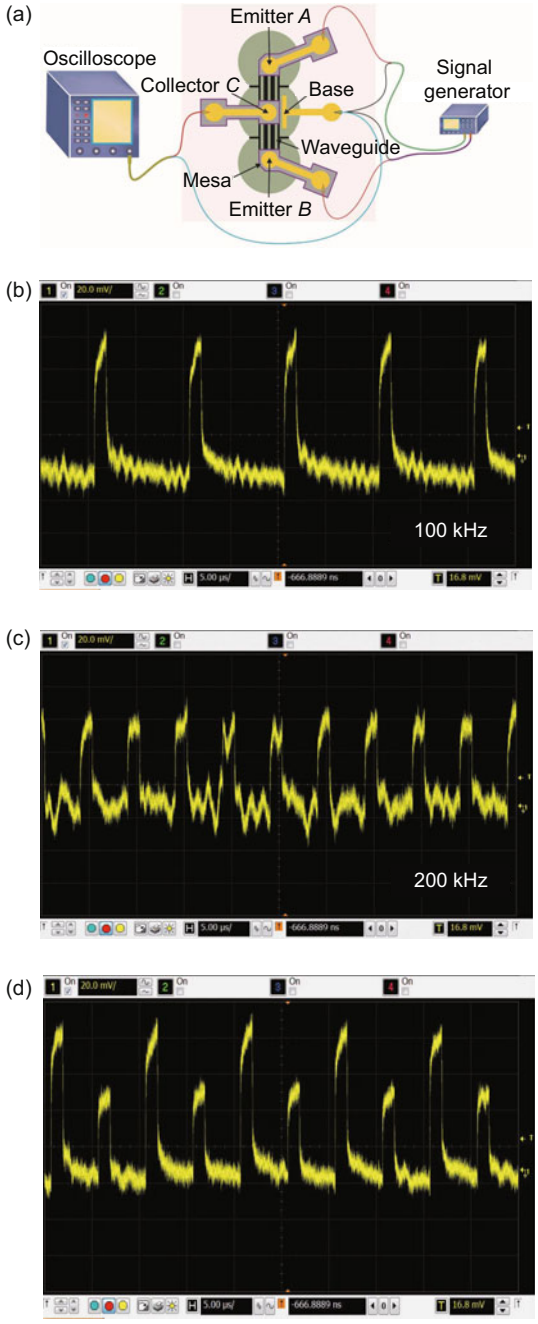

Fig. 4 Schematic of on-chip optical interconnect (a), the received signal when emitter *A* operates and emitter *B* is off (b), the received signal when emitter *A* is off and emitter *B* is turned on (c), and the received signal when both emitters operate synchronously (d) (References to color refer to the online version of this figure)

at different modulation frequencies to differentiate various output states of the proposed device. When emitter B is turned off, emitter A is driven at 3.5 V to modulate the emitted light as a square wave signal at 100 kHz with a 12.5% duty cycle. Fig. 4b shows the received electric signals at the collector. Then, emitter B is driven at 2.7 V to modulate the emitted light as a square wave at 200 kHz with a 25% duty cycle while emitter A is turned off. Fig. 4c shows the electric signals received at the collector. Because the modulation frequency is different, the two output signals can be clearly distinguished. Fig. 4d shows the electric signals received by photodiode C when both emitters operate synchronously to modulate the emitted light. The device can transform separable states into a superposition of states via the emitted light. Furthermore, there is no output signal when both emitters are turned off. The experimental results indeed demonstrate that the integrated optoelectronic device is operating properly to achieve the four output combinations for on-chip optical interconnect using visible light.

The proposed device can be used as two collectors, a common emitter, and a common base when device C operates under LED mode, and devices A and B are considered as two photodiodes. Fig. 5a shows the measured photocurrent of collector A with the bias voltage in the range of -4 to 2 V when the injection current is applied to emitter C at levels

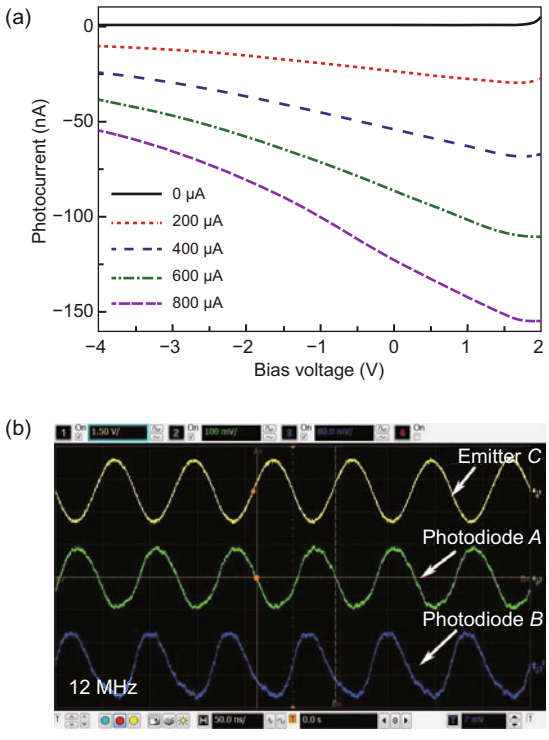

Fig. 5 The measured photocurrent of collector *A* when emitter *C* is injected with the current levels ranging from 0 to 800 μA (a), and the received signals for 1 × 2 in-plane data transport (b)

ranging from 0 to 800 μA. The induced photocurrent is increased with an increasing injection current of emitter C. Fig. 5b illustrates the received signals when emitter C is driven at 3.0 V to modulate the emitted light as a 12-MHz sinusoid. The experimental results demonstrate that the proposed device can realize the 1×2 in-plane data transport using visible light.

4 Conclusions

In summary, a wafer-level technique is developed for the realization of the on-chip photonic integration of an emitter, waveguide, and photodiode on a single chip. The proposed optoelectronic device consists of two emitters, a common collector, and a common base, and suspended waveguides are used for light coupling. The experimental results confirm that the integrated optoelectronic device can simultaneously obtain light emission, transmission, and photodetection, which potentially benefits many important applicational scenarios, such as advanced microscopy (Dai, 2017), real-time spectrometry (Cao *et al.*, 2016), and visible light communication (Yang *et al.*, 2017). Separable states are transferred into a superposition of states via photons rather than electrons, and the device operates properly to achieve the combination of four output states when the proposed optoelectronic device is treated as two emitters, a common collector, and a common base. The 1×2 data transport can be achieved when the device is used as two collectors, a common emitter, and a common base. The techniques developed in our experiments will be of significant importance for on-chip optical interconnect using visible light.

References

Bai, D., Wu, T., Li, X., *et al.*, 2016. Suspended GaN-based nanostructure for integrated optics. *Appl. Phys. B*, **122**(1):1-7. https://doi.org/10.1007/s00340-015-6293-8

Brubaker, M.D., Blanchard, P.T., Schlager, J.B., *et al.*, 2013. On-chip optical interconnects made with gallium nitride nanowires. *Nano Lett.*, **13**(2):374-377. https://doi.org/10.1021/nl303510h

Cai, W., Gao, X., Yuan, W., *et al.*, 2016a. Integrated p-n junction InGaN/GaN multiple-quantum-well devices with diverse functionalities. *Appl. Phys. Expr.*, **9**(5):052204. https://doi.org/10.7567/APEX.9.052204

Cai, W., Yang, Y., Gao, X., *et al.*, 2016b. On-chip integration of suspended InGaN/GaN multiple-quantum-well devices with versatile functionalities. *Opt. Expr.*, **24**(6): 6004-6010. https://doi.org/10.1364/OE.24.006004

Cao, X., Yue, T., Lin, X., *et al.*, 2016. Computational snapshot multispectral cameras: toward dynamic capture of the spectral world. *IEEE Signal Process. Mag.*, **33**(5): 95-108. https://doi.org/10.1109/MSP.2016.2582378

Chen, R., Tran, T.T.D., Ng, K.W., *et al.*, 2011. Nanolasers grown on silicon. *Nat. Photon.*, **5**(3):170-175. https://doi.org/10.1038/nphoton.2010.315

Dai, Q., 2017. Functional imaging of one million neurons at synaptic resolution simultaneously with a novel video-rate, sub-gigapixel microscopy at centimeter scale field-of-view, sub-micron resolution. CSH Asia Conf. on Primate Neuroscience: Perception, Cognition and Disease Models, in press.

Feng, M., Holonyak, N.Jr, Hafez, W., 2004. Light-emitting transistor: light emission from InGaP/GaAs heterojunction bipolar transistors. *Appl. Phys. Lett.*, **84**(1): 151-153. https://doi.org/10.1063/1.1637950

Jhou, Y., Chen, C.H., Chuang, R.W.K., *et al.*, 2005. Nitride-based light emitting diode and photodetector dual function devices with InGaN/GaN multiple quantum well structures. *Solid-State Electron.*, **49**(8):1347-1351. https://doi.org/10.1016/j.sse.2005.06.002

Jiang, Z., Atalla, M.R., You, G., *et al.*, 2014. Monolithic integration of nitride light emitting diodes and photodetectors for bi-directional optical communication. *Opt. Lett.*, **39**(19):5657-5660. https://doi.org/10.1364/OL.39.005657

Krost, A., Dadgar, A., 2002. GaN-based optoelectronics on silicon substrates. *Mat. Sci. Eng. B*, **93**(1):77-84. https://doi.org/10.1016/S0921-5107(02)00043-0

Kuykendall, T., Ulrich, P., Aloni, S., *et al.*, 2007. Complete composition tunability of InGaN nanowires using a combinatorial approach. *Nat. Mater.*, **6**(12):951-956. https://doi.org/10.1038/nmat2037

Li, X., Shi, Z., Zhu, G., *et al.*, 2014. High efficiency membrane light emitting diode fabricated by back wafer thinning technique. *Appl. Phys. Lett.*, **105**(3):2211-2213. https://doi.org/10.1063/1.4890859

Li, X., Zhu, G., Gao, X., *et al.*, 2015. Suspended p-n junction InGaN/GaN multiple-quantum-well device with selectable functionality. *IEEE Photon. J.*, **7**(6):1-7. https://doi.org/10.1109/JPHOT.2015.2499544

Liao, C.L., Ho, C.L., Chang, Y.F., *et al.*, 2014. High-speed light-emitting diodes emitting at 500 nm with 463-MHz modulation bandwidth. *IEEE Electron Dev. Lett.*, **35**(5):563-565. https://doi.org/10.1109/LED.2014.2304513

McKendry, J.J., Massoubre, D., Zhang, S., *et al.*, 2012. Visible-light communications using a CMOS-controlled micro-light-emitting-diode array. *J. Lightw. Technol.*, **30**(1):61-67. https://doi.org/10.1109/JLT.2011.2175090

Noda, S., Fujita, M., 2009. Light-emitting diodes: photonic crystal efficiency boost. *Nat. Photon.*, **3**(3):129-130. https://doi.org/10.1038/nphoton.2009.15

Qian, F., Li, Y., Gradečak, S., *et al.*, 2008. Multi-quantum-well nanowire heterostructures for wavelength-controlled lasers. *Nat. Mater.*, **7**(9):701-706. https://doi.org/10.1038/nmat2253

Sato, T., Takeda, K., Shinya, A., *et al.*, 2015. Photonic crystal lasers for chip-to-chip and on-chip optical interconnects. *IEEE J. Sel. Top. Quant. Electron.*,

21(6):728-737.
https://doi.org/10.1109/JSTQE.2015.2420991

Schubert, E.F., Gessmann, T., Kim, J.K., 2005. Light Emitting Diodes. John Wiley & Sons, Inc. https://dx.doi.org/10.1002/0471238961.1209070811091908.a01.pub2

Sekiya, T., Sasaki, T., Hane, K., 2015. Design, fabrication, and optical characteristics of freestanding GaN waveguides on silicon substrate. *J. Vac. Sci. Technol. B*, **33**(3):031207. https://doi.org/10.1116/1.4917487

Shokhovets, S., Himmerlich, M., Kirste, L., *et al.*, 2015. Birefringence and refractive indices of wurtzite GaN in the transparency range. *Appl. Phys. Lett.*, **107**(9):092104. https://doi.org/10.1063/1.4929976

Sun, C., Wade, M.T., Lee, Y., *et al.*, 2015. Single-chip microprocessor that communicates directly using light. *Nature*, **528**(7583):534-538. https://doi.org/10.1038/nature16454

Tchernycheva, M., Messanvi, A., de Luna Bugallo, A., *et al.*, 2014. Integrated photonic platform based on InGaN/GaN nanowire emitters and detectors. *Nano Lett.*, **14**(6):3515-3520. https://doi.org/10.1021/nl501124s

Triviño, N.V., Butte, R., Carlin, J.F., *et al.*, 2015. Continuous wave blue lasing in III-nitride nanobeam cavity on silicon. *Nano Lett.*, **15**(2):1259-1263. https://doi.org/10.1021/nl504432d

van Zeghbroeck, B., Harder, C., Meier, H.P., *et al.*, 1989. Photon transport transistor. Int. Technical Digest on Electron Devices Meeting, p.543-546. https://doi.org/10.1109/IEDM.1989.74340

Vučić, J., Kottke, C., Nerreter, S., *et al.*, 2010. 513 Mbit/s visible light communications link based on DMT-modulation of a white LED. *J. Lightw. Technol.*, **28**(24):3512-3518. https://doi.org/10.1109/JLT.2010.2089602

Wang, Y., Zhu, G., Cai, W., *et al.*, 2016. On-chip photonic system using suspended pn junction InGaN/GaN multiple quantum wells device and multiple waveguides. *Appl. Phys. Lett.*, **108**(16):162102. https://doi.org/10.1063/1.4947280

Wierer, J.J., David, A., Megens, M.M., 2009. III-nitride photonic-crystal light-emitting diodes with high extraction efficiency. *Nat. Photon.*, **3**(3):163-169. https://doi.org/10.1038/nphoton.2009.21

Yang, Y., Zhu, B., Shi, Z., *et al.*, 2017. Multi-dimensional spatial light communication made with on-chip InGaN photonic integration. *Opt. Matt.*, **66**:659-663. https://doi.org/10.1016/j.optmat.2017.03.017

Yuan, J., Cai, W., Gao, X., *et al.*, 2016. Monolithic integration of a suspended light-emitting diode with a Y-branch structure. *Appl. Phys. Expr.*, **9**(3):032202. https://doi.org/10.7567/APEX.9.032202

Zhang, Y., Oka, T., Suzuki, R., *et al.*, 2014. Electrically switchable chiral light-emitting transistor. *Science*, **344**(6185):725-728. https://doi.org/10.1126/science.1251329